Molecular Phylogenetics and Evolution 124 (2018) 137–150

Contents lists available at ScienceDirect

Molecular Phylogenetics and Evolution

journal homepage: www.elsevier.com/locate/ympev

A phylogenomic perspective on the robust capuchin monkey (*Sapajus*) radiation: First evidence for extensive population admixture across South America

Marcela G.M. Lima[a,b], José de Sousa e Silva-Júnior[b], David Černý[c], Janet C. Buckner[c], Alexandre Aleixo[b], Jonathan Chang[c], Jimmy Zheng[c], Michael E. Alfaro[c], Amely Martins[d,e], Anthony Di Fiore[d], Jean P. Boubli[f], Jessica W. Lynch Alfaro[a,g,*]

[a] Institute for Society and Genetics, University of California, Los Angeles, CA, USA
[b] Curso de Pós-Graduação em Zoologia, Universidade Federal do Pará/Museu Paraense Emílio Goeldi, Belém, PA, Brazil
[c] Department of Ecology and Evolutionary Biology, University of California, Los Angeles, USA
[d] Department of Anthropology, University of Texas at Austin, Austin, TX, USA
[e] Centro Nacional de Pesquisa e Conservação de Primatas Brasileiros, ICMBio, MMA, Brazil
[f] School of Environment and Life Sciences, University of Salford, UK
[g] Department of Anthropology, UCLA, Los Angeles, CA, USA

ARTICLE INFO

Keywords:
Neotropical primates
Phylogeny
Single nucleotide polymorphisms (SNPs)
Species tree
Ultraconserved elements (UCEs)

ABSTRACT

Phylogenetic relationships amongst the robust capuchin monkeys (genus *Sapajus*) are poorly understood. Morphology-based taxonomies have recognized anywhere from one to twelve different species. The current IUCN (2017) classification lists eight robust capuchins: *S. xanthosternos*, *S. nigritus*, *S. robustus*, *S. flavius*, *S. libidinosus*, *S. cay*, *S. apella* and *S. macrocephalus*. Here, we assembled the first phylogenomic data set for *Sapajus* using ultra-conserved elements (UCEs) to reconstruct a capuchin phylogeny. All phylogenomic analyses strongly supported a deep divergence of *Sapajus* and *Cebus* clades within the capuchin monkeys, and provided support for *Sapajus nigritus*, *S. robustus* and *S. xanthosternos* as distinct species. However, the UCE phylogeny lumped the putative species *S. cay*, *S. libidinosus*, *S. apella*, *S. macrocephalus*, and S. *flavius* together as a single widespread lineage. A SNP phylogeny constructed from the UCE data was better resolved and recovered *S. flavius* and *S. libidinosus* as sister species; however, *S. apella*, *S. macrocephalus*, and *S. cay* individuals were recovered in two geographic clades, from northeastern and southwestern Amazon, rather than clustering by currently defined morphospecies. STRUCTURE analysis of population clustering revealed widespread admixture among *Sapajus* populations within the Amazon and even into the Cerrado and Atlantic Forest. Difficulty in assigning species by morphology may be a result of widespread population admixture facilitated through frequent movement across major rivers and even ecosystems by robust capuchin monkeys.

1. Introduction

Robust capuchin monkeys (*Sapajus*) comprise a widespread Neotropical primate genus found from the Colombian Llanos to the Guianas and throughout the Amazon basin, as well as in the Atlantic Forest, Cerrado, Caatinga, and Pantanal biomes of South America, to as far south as northern Argentina (Rylands et al., 2013). Robust capuchins are true habitat generalists, with an incredible diet breadth compared to other Neotropical primates. While fruit and insects form the bulk of their diets, their robust jaw morphology, coupled with behavioral adaptations for tool use and manipulative and extractive foraging, together allow them to exploit encased and hidden foods unavailable to most other non-human animals (Fragaszy et al., 2004; Lynch Alfaro et al., 2012b). This in turn allows them to occupy habitats usually inhospitable to primates.

Current primate taxonomy separates robust (*Sapajus*) and gracile (*Cebus*) capuchin monkeys in two genera, while earlier taxonomists lumped all capuchins into one genus, *Cebus*, despite recognizing morphological differences between the two types. For example, Elliot (1913) created a taxonomic key that divided the genus *Cebus* into

* Corresponding author at: Institute for Society and Genetics, 621 Charles E. Young Dr. South, 3323E Life Sciences Bldg., University of California, Los Angeles, Los Angeles, CA 90095 USA.
E-mail addresses: marcela_gml@yahoo.com.br (M.G.M. Lima), jlynchalfaro@g.ucla.edu (J.W. Lynch Alfaro).

https://doi.org/10.1016/j.ympev.2018.02.023
Received 25 June 2017; Received in revised form 6 January 2018; Accepted 23 February 2018
Available online 12 March 2018

Table 1
Taxonomies of robust capuchin monkeys.

Elliot (1913)	Hershkovitz (1949)	Cabrera (1957)	Hill (1960)	Groves (2001, 2005)	Silva-Júnior (2001, 2005)	Rylands et al. (2013)
Cebus apella	*Cebus apella*	*Cebus apella*	*Cebus apella*	*Cebus apella*	*Cebus (Sapajus) apella*	*Sapajus apella*
Cebus fatuellus		*C. a. apella*	*C. a. apella*	*C. a. apella*	*Cebus (Sapajus) macrocephalus*	*Sapajus macrocephalus*
C. f. fatuellus		*C. a. margaritae*	*C. a. margaritae*	*C. a. fatuellus*	*Cebus (Sapajus) libidinosus*	*Sapajus libidinosus*
C. f. peruanus		*C. a. macrocephalus*	*C. a. fatuellus*	*C. a. macrocephalus*	*Cebus (Sapajus) cay*	*Sapajus cay*
Cebus macrocephalus		*C. a. libidinosus*	*C. a. peruanus*	*C. a. peruanus*	*Cebus (Sapajus) nigritus*	*Sapajus nigritus*
Cebus libidinosus		*C. a. paraguayanus*	*C. a. tocantinus*	*C. a. tocantinus*	*Cebus (Sapajus) robustus*	*S. n. nigritus*
Cebus azarae		*C. a. pallidus*	*C. a. macrocephalus*	*C. a. margaritae*	*Cebus (Sapajus) xanthosternos*	*S. n. cucullatus*
C. a. azarae		*C. a. xanthosternos*	*C .a. libidinosus*	*Cebus libidinosus*		*Sapajus robustus*
C. a. pallidus		*C. a. versutus*	*C. a. cay*	*C. l. libidinosus*		*Sapajus xanthosternos*
Cebus frontatus		*C. a. nigritus*	*C. a. pallidus*	*C. l. pallidus*		*Sapajus flavius*
Cebus variegatus		*C. a. vellerosus*	*C. a. frontatus*	*C. l. paraguayanus*		
Cebus versuta		*C. a. robustus*	*C. a. xanthosternos*	*C. l. juruanus*		
Cebus cirrifer			*C. a. nigritus*	*Cebus nigritus*		
Cebus crassiceps			*C. a. robustus*	*C. n. nigritus*		
Cebus caliginosus			*C. a. magnus*	*C. n. robustus*		
Cebus vellerosus			*C. a. juruanus*	*C. n. cucullatus*		
			C. a. maranonis	*Cebus xanthosternos*		

'tufted' and 'non-tufted' groups based on whether hair tufts were present on the frontal region of the head. Hershkovitz (1949) cemented a general consensus about the validity of this division, with just one species (*Cebus apella* Linnaeus, 1758) recognized for the tufted group. Hill (1960) also considered all robust or tufted capuchins to be a single cosmopolitan species, *Cebus apella*. Groves (2001, 2005) divided capuchins in two species groups: (1) the *C. capucinus* group, comprising *C. capucinus*, *C. albifrons*, *C. olivaceus*, and *C. kaapori*; and (2) the *C. apella* group, with *C. apella*, *C. libidinosus*, *C. nigritus*, and *C. xanthosternos* (Table 1). Silva-Júnior (2001) separated the tufted or robust capuchins as a different subgenus (*Sapajus*) from the non-tufted or gracile capuchins (*Cebus*) based on distinct cranial, post-cranial, and pelage morphology; he emphasized that *Sapajus* skull and mandible are more robust than that of *Cebus*, because of differences in feeding ecology. Subsequently, genetic research validated the separation of robust and gracile capuchins as two distinct and diverse clades using mitochondrial (Lynch Alfaro et al., 2012a; Lima et al., 2017) and a combination of mtDNA and nuclear (Perelman et al., 2011) markers. Two *Alu* elements also provide strong evidence for the monophyly of robust versus gracile capuchins: *Alu* element S49P is present in *Sapajus* but not *Cebus* (Viana et al., 2015), and the AluSc8 insertion is found in *Cebus* but not *Sapajus* (Martins Jr. et al., 2015). A recent review justified the splitting capuchins into two genera (*Cebus* for gracile capuchins and *Sapajus* for robust capuchins) based on the distinctive morphology, biogeographic history, behavior, and ecology of each type (Lynch Alfaro et al., 2012b).

Taxonomists have also disagreed about the number of species of extant robust capuchins based on morphology (Table 1). Elliot (1913) recognized twelve species of robust capuchins, but Cabrera (1957) and Hill (1960), as noted above, placed all robust forms into one species, *Cebus apella*, while retaining 11 and 16 subspecies, respectively. For the four decades between 1960 and 2000, most researchers considered all robust capuchins to belong to a single species irrespective of place of origin and usually without regard for subspecies designations (e.g. Cole, 1992; Daegling, 1992; Ford and Hobbs, 1996; Masterson, 1997; Wright, 2005a; 2005b, 2007), leading to obfuscation of species or population differences within the robust capuchin literature (see Lynch Alfaro et al., 2014 for discussion). However, Torres de Assumpção (1983) pointed to distinct geographical variation in morphology among robust capuchin populations within Brazil, especially within the Atlantic Forest. More recent morphological analyses have provided evidence for multiple *Sapajus* species (Groves, 2001, 2005; Silva-Júnior, 2001, 2002, 2005; Rylands et al., 2005, 2012, 2013; Rylands and Mittermeier, 2009). The robust capuchin group is now considered by most taxonomists to comprise between four and eight species (Silva-Júnior, 2001; Groves, 2001; Rylands and Mittermeier, 2009; Rylands et al., 2005, 2012, 2013). The IUCN (2017) currently recognizes eight distinct species: *Sapajus flavius*, the blonde capuchin; *S. xanthosternos*, the yellow-breasted capuchin; *S. robustus*, the robust tufted capuchin; *S. nigritus*, the black-horned capuchin; *S. apella*, the brown capuchin; *S. macrocephalus*, the large-headed capuchin; *S. cay*, Azara's capuchin; and *S. libidinosus*, the bearded capuchin.

Recent biogeographic analyses based on mitochondrial DNA suggest that the age of the radiation of extant robust capuchins is about 2.5 My, with diversity accumulating first in the Atlantic Coastal Forest of Brazil and a recent expansion of robust capuchins throughout the Amazon Basin and Cerrado, Caatinga, and Central Grasslands in the last 500,000 years (Lynch Alfaro et al., 2012a; Lima et al., 2017). These analyses suggest that while the Atlantic Forest populations are relatively old and distinct and can be divided into up to four different species, the forms from the Amazon and savanna-like biomes are better considered to be members of a highly polymorphic single species or species complex (Lima et al., 2017).

Here, we use phylogenomic markers – ultraconserved elements (UCEs) (Faircloth et al., 2013) – to infer the phylogeny of robust capuchin monkeys, and to assess the evidence for congruence with species delineation based on morphology and mitochondrial markers. The UCE approach has been used successfully to answer historically contentious taxonomic questions (McCormack et al., 2012; Crawford et al., 2012), including Pleistocene radiations (McCormack et al., 2015; but see Giarla et al. 2015 for challenges in estimating a bifurcating tree even using UCEs when there is a rapid and recent radiation). Previous studies using nuclear markers for capuchin phylogeny have used a limited number of taxa and have also used captive individuals with unknown provenance as species exemplars (i.e. Perelman et al., 2011, Springer et al., 2012). This study marks the first test of robust capuchin phylogeny using phylogenomic markers to analyze genetic relationships across species-representative individuals from known provenance. We use SNP (Single Nucleotide Polymorphisms) data from the UCE results to refine our understanding of robust capuchin diversification in the Pleistocene, as this technique has been used successfully to elucidate phylogeny across a similar geologic time frame (McCormack et al., 2015).

2. Material and methods

2.1. Samples, DNA extraction and sequencing

We sampled 61 individuals from eight species of the genus *Sapajus* from 58 localities distributed throughout the Atlantic Forest, Amazon, Caatinga, Cerrado and Pantanal habitats in South America (Fig. 1, Table 2, Supplementary Table 1). Note that our study extends the *S. macrocephalus* morphotype to the east of the Madeira River, into the

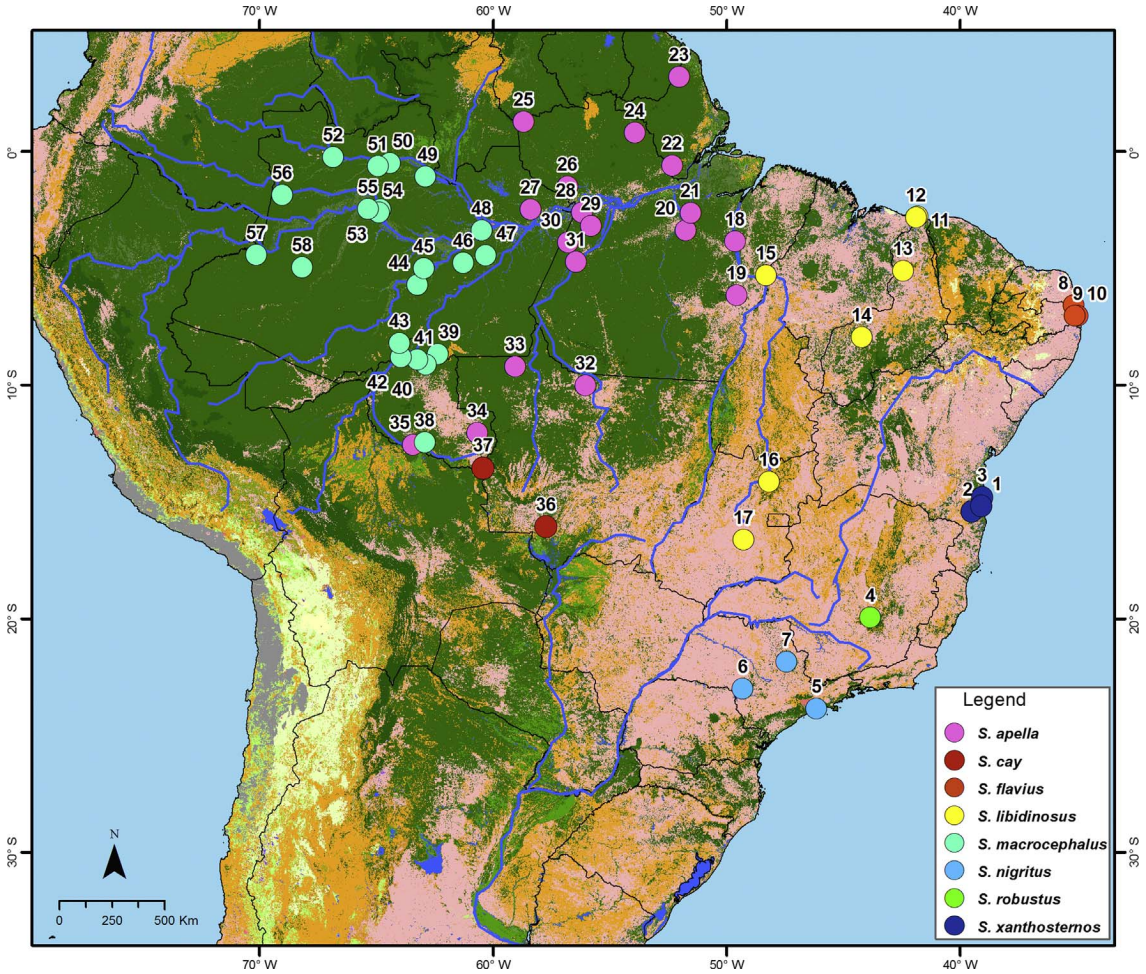

Fig. 1. Map showing the sampled localities for *Sapajus*. Sample numbers correspond to those in Table 2 and Supplementary Table 1. Species names are based on IUCN (2017).

Brazilian state of Rondônia. We also sampled 7 individuals from 5 species of gracile capuchins, genus *Cebus*. Total genomic DNA was extracted from muscle and blood samples using the Qiagen DNeasy Blood & Tissue Kit, according to the manufacturer's protocol. Library preparation, sequence capture, and sequencing of ultraconserved elements were performed by RAPiD Genomics (Gainesville, FL, USA). Samples were quantified, normalized and sheared to an average fragment length of 350 base pairs (bp) for library preparation. Samples were dual-indexed with unique i5 and i7 8bp indexes. Libraries were then pooled with equimolar concentrations, and the target sequence was captured using a custom set of 4715 probes targeting approximately 2300 UCE loci. Capture libraries were then pooled in equimolar concentrations for multiplexed dual-end (2×100bp) sequencing on the Illumina HiSeq 2500 v4 platform.

2.2. Sequence read quality control, assembly and UCE identification

We performed quality control using the software tool Trimmomatic 0.32.1 (Bolger et al., 2014), which trimmed sequences for adapter contamination, barcodes, and low-quality regions using the parallel wrapper script in Illumiprocessor 2.0.6 (Faircloth, 2013) (https://github.com/faircloth-lab/illumiprocessor). We assembled the contigs for each sample using the Trinity software package (v 02-25-2013) with default parameters using Phyluce 1.5.0 (Faircloth, 2016). We matched our assembled contigs to 4715 UCE loci custom-designed probe set using phyluce_assembly_match_contigs_to_probes integrating LASTZ 1.02.00 (Harris, 2007) from Phyluce 1.5.0 (Faircloth, 2016) to remove any contigs that did not match probes or that matched multiple probes from different UCE loci. We aligned contigs using the program phyluce_align_seqcap_align with MAFFT 7.271 (Katoh and Standley, 2013) in Phyluce 1.5.0 (Faircloth, 2016).

2.3. Phylogenomic analyses

For our phylogenomic analyses, we used a concatenated data set in a single alignment constructed in Phyluce 1.5.0 (Faircloth et al., 2012; Faircloth, 2016). The alignment included greater than 75% of taxa present for each UCE locus totaling 1838 UCEs. We performed phylogenetic tree reconstruction under maximum likelihood (ML) in RAxML 8.0.19 (Stamatakis, 2014), using a GTRGAMMA model of nucleotide substitution with 100 replicate searches to identify the optimal tree and node support was assessed via 1000 non-parametric bootstrap replicates. Before running these analyses we used PartitionFinder (Lanfear et al., 2012) to find the best partitioning scheme. We considered each UCE as a data block and enabled hcluster (Lanfear et al., 2014) with equal weights. To evaluate the fit of each model we used the Bayesian information criterion (BIC).

2.4. SNPs analyses

Upon identifying the target UCE loci, we computed the coverage at each base of each contig using a python wrapper included in Phyluce 1.5.0 (phyluce_assembly_get_trinity_coverage_for_uce_loci). We then employed a *de novo* SNPs-calling approach by aligning all raw reads for *Sapajus* samples against our sample of *S. robustus*, the reference sample with the highest coverage across all UCE loci enriched. This method

Table 2
List of samples, locality data and resulting UCE data.

Map	Species	Latitude	Longitude	Trimmed reads	Contigs Assembled	Avg Len	UCE contigs	Avg Len	UCE contigs coverage (x)
1	*S. xanthosternos*	−15.17	−39.07	2,681,597	3274	388.5	1970	408	11.4
2	*S. xanthosternos*	−15.41	−39.5	2,843,593	3661	382.9	1995	413.9	12.5
3A	*S. xanthosternos*	−14.79	−39.05	3,196,673	3802	392.4	1998	441.5	12.3
3B	*S. xanthosternos*	−14.79	−39.05	3,521,726	4275	389	2003	459	13.1
4	*S. robustus*	−19.95	−43.85	4,538,948	5198	373.5	2044	466.4	16.8
5	*S. nigritus*	−23.86	−46.14	2,762,021	3471	389.6	1825	409	9.7
6	*S. nigritus*	−23	−49.32	946,881	1937	328	1450	284.3	7.1
7	*S. nigritus*	−21.85	−47.43	1,860,595	2897	460.7	1822	392.8	8.6
8	*S. flavius*	−6.56	−35.13	2,713,906	3096	402.9	1971	421.9	11
9	*S. flavius*	−7.01	−34.96	4,787,966	5150	363.5	2031	457.3	14.6
10	*S. flavius*	−7.02	−35.09	2,877,922	3601	397.1	2000	435.4	13.2
11	*S. libidinosus*	−2.77	−41.81	2,764,451	3430	381.4	1941	402.1	10.3
12	*S. libidinosus*	−2.8	−41.87	4,348,317	5094	357.8	2025	435.7	13.3
13	*S. libidinosus*	−5.09	−42.43	2,612,178	3208	417.7	1890	357.4	9.3
14	*S. libidinosus*	−7.93	−44.2	3,068,523	3551	395.7	1986	421.6	10.9
15	*S. libidinosus*	−5.28	−48.3	3,303,530	3885	372.6	1966	401.2	11.2
16	*S. libidinosus*	−14.14	−48.17	3,381,894	3603	377.5	1965	399.5	10.4
17	*S. libidinosus*	−16.6	−49.26	3,301,692	3884	372.2	1989	410.1	11.3
18A	*S. apella*	−3.83	−49.64	3,541,159	3793	380.3	1991	423.3	11.8
18B	*S. apella*	−3.83	−49.64	2,980,533	3534	379.2	1961	408.5	10.6
19	*S. apella*	−6.15	−49.56	1,908,769	2828	416.6	1920	418.8	10
20	*S. apella*	−3.36	−51.74	3,391,742	3723	382.9	1996	418.8	11.6
21	*S. apella*	−2.61	−51.54	5,485,708	6170	355.6	2034	487.9	15.5
22	*S. apella*	−0.58	−52.33	1,311,929	2137	373.2	1621	326.1	6.9
23	*S. apella*	3.22	−52.03	1,757,726	2338	384	1728	356	7.5
24	*S. apella*	0.83	−53.93	2,781,762	2805	352.7	1754	338.4	8.3
25	*S. apella*	1.29	−58.7	2,130,450	2604	384.5	1839	366.7	8.7
26	*S. apella*	−1.49	−56.8	1,572,934	2413	385.4	1773	360.6	7.8
27	*S. apella*	−2.47	−58.4	3,571,090	3780	385.6	1999	420.9	12.3
28	*S. apella*	−2.6	−56.18	2,394,355	3227	394.6	1966	412	11.6
29	*S. apella*	−3.18	−55.8	1,890,413	2709	391.7	1884	383	9.3
30	*S. apella*	−3.88	−56.78	1,276,241	2039	363.8	1520	325.7	6.5
31	*S. apella*	−4.71	−56.44	1,746,336	2515	379	1812	359.1	8.2
32	*S. apella*	−10	−56.04	1,791,793	2450	394.9	1741	352.4	7.5
33	*S. apella*	−9.2	−59.06	2,103,015	2895	365.5	1886	359.4	9.4
34	*S. apella*	−12.03	−60.67	2,339,872	3027	382.9	1898	377.2	9.3
35	*S. apella*	−12.56	−63.44	3,883,141	4558	380.2	2024	447.3	13.4
36	*S. cay*	−16.06	−57.72	1,624,662	2588	373.8	1765	350.1	7.6
37	*S. cay*	−13.52	−60.43	2,361,492	2991	384.1	1933	388	9.6
38	*S. macrocephalus*	−12.45	−62.92	2,986,344	3335	381.3	1967	399.7	10.5
39	*S. macrocephalus*	−8.67	−62.37	2,962,283	3477	370.5	1952	392.7	10.5
40	*S. macrocephalus*	−9.1	−62.88	2,222,218	2882	376.6	1900	371.4	9.3
41	*S. macrocephalus*	−8.89	−63.24	3,054,313	3411	372.6	1963	391.9	10.3
42	*S. macrocephalus*	−8.8	−63.95	1,459,387	2148	361.4	1570	324.7	7
43	*S. macrocephalus*	−8.19	−64.02	2,196,025	2741	375.9	1881	365.5	8.9
44	*S. macrocephalus*	−5.69	−63.24	3,840,307	4395	363	2009	422.6	12.8
45A	*S. macrocephalus*	−4.99	−62.96	3,199,632	3780	383.4	1994	433.9	12
45B	*S. macrocephalus*	−4.99	−62.96	1,163,783	2218	355.6	1650	326.1	7.3
46	*S. macrocephalus*	−4.75	−61.28	2,351,064	3072	394.7	1932	379.2	11.1
47	*S. macrocephalus*	−4.44	−60.32	2,219,015	2938	374.6	1922	366.9	9.8
48	*S. macrocephalus*	−3.37	−60.48	1,876,035	2707	367.5	1841	343.6	8.6
49	*S. macrocephalus*	−1.05	−62.89	2,044,899	2699	387.1	1871	372.3	9.2
50	*S. macrocephalus*	−0.48	−64.41	2,723,327	3234	385	1922	398.4	10.2
51	*S. macrocephalus*	−0.61	−64.92	3,169,376	3983	350	1980	379.2	11.5
52	*S. macrocephalus*	−0.23	−66.85	2,105,443	2681	383	1868	368.8	9.1
53	*S. macrocephalus*	−2.47	−64.83	3,117,247	3756	419.3	2015	484.5	12.5
54	*S. macrocephalus*	−2.59	−64.89	2,484,843	2946	408.9	1937	424.5	9.8
55	*S. macrocephalus*	−2.45	−65.36	1,918,138	2692	401.6	1869	401.9	9.1
56	*S. macrocephalus*	−1.84	−69.03	2,085,573	2716	394.7	1878	391.5	8.9
57	*S. macrocephalus*	−4.4	−70.14	3,522,837	4000	369.4	1992	422.5	12.2
58	*S. macrocephalus*	−4.94	−68.17	4,107,017	4659	370.7	2003	453.9	13.4
–	*C. unicolor*	−9.22	−66.74	2,057,387	3279	394.2	1902	371.2	10.5
–	*C. o. castaneus*	−0.58	−52.33	2,107,696	3145	402	1836	376.3	8.6
–	*C. o. castaneus*	1.84	−52.74	1,401,630	2151	373.9	1483	316.4	6.7
–	*C. kaapori*	−2.33	−46.08	2,885,841	3593	443.1	1983	425.9	10.5
–	*C. capucinus*	10.95	−84.55	3,954,729	4702	419.8	2026	450.1	13.9
–	*C. capucinus*	10.88	−85.78	508,807	1162	288.9	891	267.2	5
–	*C. albifrons*	−2.59	−64.89	3,111,458	3951	391	1995	428.9	12.2

integrated BWA v0.7.7-1 (Li and Durbin, 2009) and PICARD v1.106-0 (http://picard.sourceforge.net,) to output *de novo* alignments in bam format, repair any formatting violations, add read group header information, and mark duplicates in each bam. We then merged all resulting bams into one file, realigning the data and calling SNPs and indels using GATK v3.5-0-g36282e4 (McKenna et al., 2010). To ensure high-quality SNPs in downstream analyses, we hierarchically filtered the data according to stringent quality and validation parameters,

excluding SNPs with QUAL scores under 25, low variant confidence, and poor validation. Finally, the resulting VCF was passed through VCFTOOLS v0.1.14 (Danecek et al., 2011) to remove all loci that missed SNP calls for over 25% of all 61 samples. We performed the same SNPs-calling approach for the entire *Sapajus-Cebus* data set (n = 68) for use in the SVDquartets species tree analysis (see below). We also used the 'thin' feature in Phyluce to create a dataset of unlinked SNPs, totaling 1910 for the *Sapajus* dataset, for STRUCTURE analyses (see below).

We performed a maximum likelihood (ML) analysis in RAxML 8.0.19 (Stamatakis, 2014) using the full SNPs dataset, assuming a general time reversible model of rate substitution and gamma-distributed rates among sites (GTRGAMMA). We performed 100 replicate searches to identify the optimal tree and node support was assessed via 1000 non-parametric bootstrap replicates.

Finally, we estimated a species tree using SVDquartets analyses (Singular Value Decomposition Scores for Species Quartets; Chifman and Kubatko, 2014) implemented in PAUP* v4.0a159 (Swofford, 2002). This method infers quartets based on summaries of SNPs in a concatenated sequence matrix of species using a coalescent model. We randomly sampled 10 million quartets from the data matrix to infer a species tree.

2.5. Population genetic analyses

To better understand the structure of capuchin genetic diversity and assess the degree of gene flow across putative species, we performed population structure analyses, using the model-based Bayesian clustering method in STRUCTURE v.2.3.4 (Pritchard et al., 2000) to infer the optimal number of genetic populations (K) as suggested by the SNPs data. We used two models to infer population structure from our sample of *Sapajus* SNPs from the UCE dataset. Both used the Markov Chain Monte Carlo (MCMC) approach, which groups individuals into K populations based on their genotype, without using information about their provenance or species assignation based on morphology.

In the first model, we used NO ADMIXTURE and correlated allele frequencies with the unlinked SNPs dataset. We evaluated the hypotheses K = 1–9, with 3 runs of each number of clusters, with 10,000 iterations of burn-in followed by 100,000 iterations of MCMC. We identified the most likely number of populations using the delta K method (Evanno et al., 2005) as implemented in STRUCTURE HARVESTER 0.6.94 (Earl and vonHoldt, 2012). We also evaluated substructure among the main clusters.

In the second model, we used ADMIXTURE and correlated allele frequencies with the full *Sapajus* SNPs dataset. We evaluate the hypotheses K = 1–9, with 3 runs of each number of clusters, with 10,000 iterations of burn-in followed by 100,000 iterations of MCMC. Again, we identified the most likely number of populations using the delta K method (Evanno et al., 2005) as implemented in STRUCTURE HARVESTER 0.6.94 (Earl and vonHoldt, 2012).

2.6. Divergence dating analyses

We inferred an evolutionary timescale for the capuchin radiation using two methods to test whether divergence times for *Sapajus* and *Cebus* based upon the UCE data were concordant with timescales based upon earlier mitochondrial and nuclear genetic data sets (Perelman et al., 2011; Springer et al., 2012; Lima et al., 2017). Exploratory analyses in BEAST 1.8.4 revealed that analyses using the full data set were not computationally tractable. To identify the subset of UCE sites that would be most useful in capturing shallow divergences, we re-analyzed the 75% complete dataset in PartitionFinder 2 (Lanfear et al., 2017) using the *k*-means algorithm described by Frandsen et al. (2015) and BIC as the model selection method. We identified the fastest-evolving partition based on the rate multipliers reported in auxiliary files generated using the "–save-phylofiles" flag. This partition, totaling 15,332 sites, was then used to conduct a time tree analysis using BEAST 1.8.4 (Drummond et al., 2012).

We used the birth-death branching process (Gernhard, 2008) with default hyperpriors placed on the growth rate and relative death rate hyperparameters to generate the joint prior distribution on tree topology and node heights. An uncorrelated lognormal relaxed clock was used to model the distribution of branch rates across the tree. In order to constrain the branch rate distribution to biologically realistic values, we placed a lognormal hyperprior with a mean of 0.005 (in real space) and a standard deviation of 1 on the ucld.mean hyperparameter (initial value of 0.005), and we assigned a truncated exponential distribution with support from 0 to 1 and a mean of 0.3 to the ucld.stdev hyperparameter (initial value of 0.1). GTR + Γ was specified as the nucleotide substitution model; all free parameters were assigned default priors, the base frequencies were estimated rather than fixed, and the gamma rate heterogeneity distribution was discretized into 4 categories.

We ran the analysis under the fixed topology operator mix as specified in BEAUTi v1.8.4 (Drummond et al., 2012), with the tuning of the ucld.mean and ucld.stdev operators set to 0.9 and their weight increased to 6.0. All remaining operators were kept at their default values. The topological constraint we employed was based on the species tree inferred with SVDquartets (see below) and supplemented with ten outgroups, including one cebid (*Saimiri boliviensis* extracted from GCA_000235385.1) and one aotid (*Aotus nancymaae* extracted from GCA_000952055.1) from GenBank, as well as one callitrichid (*Callithrix jacchus*) and seven catarrhines from Faircloth et al. (2012). While the relationships among the catarrhine outgroups were constrained to correspond to the generally accepted phylogeny of the Simiiformes (Perelman et al., 2011; Springer et al., 2012), the interrelationships of *Aotus*, *Callithrix*, *Saimiri*, and the rest of Cebidae have been controversial (Perez and Rosenberger 2014). We therefore subsampled the 75% and 95% complete alignments down to the BEAST taxon set of 21 species, and ran unpartitioned RAxML and ExaBayes analyses on both of the reduced datasets. All the four analyses agreed on a topology uniting *Aotus* and *Callithrix* as the sister group to a clade including

Table 3
Fossil calibrations used for divergence time estimation (see Fig. 7 for node labels).

Calibrated node	Divergence	Fossil	Reference	Min (Ma)	Max (Ma)	Mean (BEAST)	*c* (MCMCTree)
1	Hominina/*Pan*	*Ardipithecus kadabba*	Haile-Selassie (2001)	5.1	16	3.639	0.168
4	Hominidae/Hylobatidae	*Sivapithecus* sp.	Kappelman et al. (1991)	11.6	28.5	5.641	0.115
5	*Papio/Macaca*	*Macaca libyca*	Köhler et al. (2000)	5.5	23	5.842	0.250
6	Hominoidea/Cercopithecidae	*Afropithecus turkanensis*	Young and MacLatchy (2004)	20.55	37.3	5.591	0.064
7	*Aotus/Callithrix*	*Patasola magdalenae*; *Lagonimico conclucatus*	Kay (2015) (minimum) Bloch et al. (2016) (maximum)	13.4	21.1	2.570	0.045
18	*Saimiri*/other Cebidae	*Neosaimiri fieldsi*	Kay (2016) (minimum); Bloch et al. (2016) (maximum)	12	21.1	3.038	0.060
19	Callitrichidae/Cebidae (*sensu* Rylands et al. (2012))	*Patasola magdalenae*; *Lagonimico conclucatus*	Kay (2015) (minimum); Springer et al. (2012) (maximum)	13.4	28.5	5.041	0.089
20	Catarrhini/Platyrrhini	*Aegyptopithecus zeuxis*	Benton and Donoghue (2007)	28.3	56	9.246	0.077

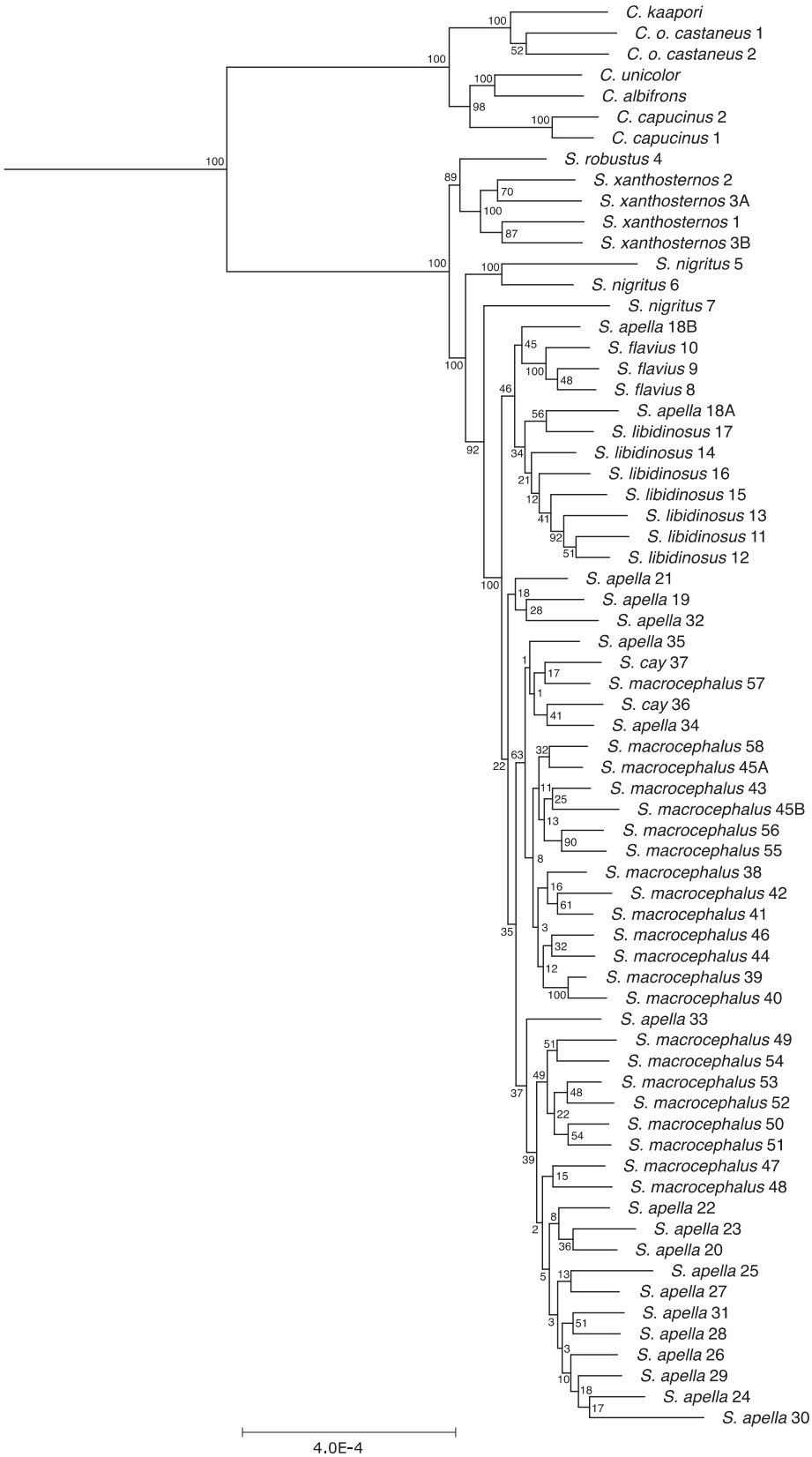

Fig. 2. Maximum likelihood (RAxML) 75% phylogeny for UCE data. Numbers at each node represent percentages from the bootstrap values (based on 1000 replicates). Sample numbers correspond to those in Table 2 and Fig. 1.

Saimiri, *Cebus*, and *Sapajus*.

To calibrate the tree, we used the fossil dates previously employed by Springer et al. (2012) that were applicable to our restricted taxon sample (Table 3). We updated the calibrations assigned to nodes 7 and 18 by using the more precise stratigraphic ranges given by Kay (2015) for the lower bounds (based on *Patasola* and *Neosaimiri*, respectively) and by basing their upper bounds on *Panamacebus*, the recently described oldest known crown cebid (Bloch et al. 2016). Each calibration point was assigned an offset exponential density such that the upper bound specified by Springer et al. (2012) corresponded to the 95th percentile of the distribution. In contrast to the uniform densities utilized by Springer et al. (2012), exponential distributions have the advantage of concentrating most probability mass close to the lower bound.

The Markov chain Monte Carlo analysis was run for 400 million generations, sampling every 1000 generations and removing the initial 10% of samples as burnin. We assessed convergence of the chain using the effective sample sizes (ESS) reported for each parameter in Tracer 1.6.0 (Rambaut et al., 2013) by ensuring that all the ESS values exceeded 200. The posterior distribution of time trees was summarized into a maximum clade credibility tree using TreeAnnotator 1.8.4 (Rambaut and Drummond, 2015).

To assess the sensitivity of the results to the choice of dating method, we performed an additional analysis using MCMCTree 4.9a from the PAML package (Yang, 2007). First, we used BASEML (also included in the PAML package) to estimate the substitution rate in units of substitutions per 10 million years. The analysis was run under the strict clock model with a single root calibration set to 37.55 Ma (the mean of the offset exponential distribution with a minimum of 28.3 Ma and a 95th percentile of 56 Ma). We set the shape parameter of the gamma prior on the mean substitution rate (rgene_gamma) to 2, with the rate parameter set to 159.94 so that the mean of the prior would equal the estimated substitution rate rescaled in units of substitutions per million years. The prior on log rate variance (sigma2_gamma) was assigned a shape of 1 and a rate of 10, which is roughly equivalent to the corresponding prior in BEAST (ucld.stdev).

We used the birth-death tree prior and set the speciation and extinction rate hyperparameters equal to 0.1. The sampling proportion hyperparameter was assigned a value of 0.06, obtained by dividing the number of species included in the analysis (21) by the total species richness of the Simiiformes as reported by Rylands and Mittermeier (2014). We employed the HKY85 + Γ substitution model with the rate heterogeneity distribution discretized into 8 categories. All calibrated nodes except the root were assigned truncated Cauchy distributions of the form $t \sim L(t_L, p, p_L, c)$, where t_L corresponded to the respective lower bounds (Table 3), p (the distance between the lower bound and the mode; Barba-Montoya et al., 2017) was set to 0 to approximate the shifted exponentials used in BEAST, p_L (the probability assigned to ages younger than the lower bound) was set to 10^{-300}, and c was calculated from the formula given in Yang (2017: 50) to ensure that 95% of probability mass fell below the upper bound. A truncated Cauchy constraint on the root age was not recognized by the program, and had to be replaced by a soft uniform prior that assigned a probability of 10^{-300} to ages younger than the lower bound and a probability of 0.05 to ages older than the upper bound.

The MCMCTree analysis consisted of two successive steps. First, we generated a temporary file with the maximum likelihood branch length estimates and the corresponding Hessian matrix calculated using BASEML (usedata = 3). We then used this temporary file to start a Markov chain Monte Carlo analysis (usedata = 2) with 5000 burnin and 10,000 post-burnin samples, sampling every 250 iterations. We used the ESS criterion in Tracer as described above to determine whether the chain had reached stationarity.

3. Results

3.1. Quality control

We sequenced a total of 178 million read pairs (mean = 2661695.4) for all samples. An average of 3309 contigs per sample (min = 1162, max = 6170) was assembled from 68 individuals (Table 2). After alignment and trimming as described above, which removed ragged edges, we recovered an average of 1882 unique contigs matching UCE loci from each sample. We produced a 75% complete data matrix containing 1838 alignments of UCE loci, which produced a concatenated matrix of 536,289 bp (average length: 298.70 bp per alignment).

3.2. Phylogenomic analyses

We recovered strong support (100) for reciprocal monophyly of the *Sapajus* and *Cebus* clades in ML analysis of the UCE sequence dataset (Fig. 2). Our analysis showed strong molecular support for three of the morphological species within the genus *Sapajus*: *S. robustus*, *S. xanthosternos*, and *S. nigritus*, all within the Atlantic Forest of Brazil. The topology of *S. nigritus* 7 in the tree can explained by admixture with *S. libidinosus* (see Population genetic structure analyses section, below). All other morphologically defined species within the genus (*S. flavius*, *S. libidinosus*, *S. apella*, *S. cay,* and *S. macrocephalus*) grouped together with high support (100) in a widely distributed clade (from the Atlantic Forest to the Amazon), but there was no support for any internal structure within this clade. Thus, the ML tree suggests three species of *Sapajus* from the Atlantic Forest of Brazil (*S. robustus, S. xanthosternos* and *S. nigritus*) plus an additional, widespread species of robust capuchin that encompasses morphotypes *S. flavius*, *S. libidinosus*, *S. apella*, *S. cay,* and *S. macrocephalus*.

3.3. SNPs analyses

After filtering out low quality SNP sites within the UCE sequences, we identified a total of 19,436 SNPs across all samples. We then filtered out sites with missing data and non-parsimony-informative sites to generate a 75% complete data matrix comprising a total of 11,402 informative high quality SNPs.

In contrast to the widespread clade recovered in our ML phylogenetic analysis of the UCE sequence data, our SNP-based analyses recovered two distinct widespread clades for *Sapajus* that better matched expectations based on morphology and geography (Fig. 3). McCormack et al. (2015) also found that SNPs from their UCE dataset best resolved species differentiation among scrub jays. According to McCormack et al. (2015), the better performance of SNP-based coalescent analysis over UCE-based phylogenetic analysis may be due to several factors, including that each SNP is based on more data and more stringent parameters due to the filtering for quality and coverage.

The phylogenetic tree inferred from maximum likelihood analyses using these SNPs from the UCE sequence data recovered *Sapajus xanthosternos* and *S. nigritus* (with the exception of *S. nigritus* 7, as in the ML tree) as monophyletic groups, and *S. robustus* as sister to *S. xanthosternos* (Fig. 3). Another *Sapajus* clade consisted of a monophyletic grouping of the species *Sapajus flavius* plus all *S. libidinosus* samples in a clade with *S. apella* specimens from the site of Tucuruí. A second clade comprised samples of *S. cay*, *S. apella*, and *S. macrocephalus* without any support for species groupings within the clade. Within the Amazonian forms from the widely distributed clade, we found a general division between northeastern versus southwestern Amazonian *Sapajus* (see convex polygons for Northern and Southern Amazonian clades on the map in Fig. 3). Thus, our phylogenomic SNP data provides some support for six species within the genus *Sapajus*: *S. nigritus*, *S. robustus*, *S. xanthosternos*, *S. flavius, S. libidinosus*, and an additional widespread species found in Amazonia, the Pantanal and southern savanna of Brazil

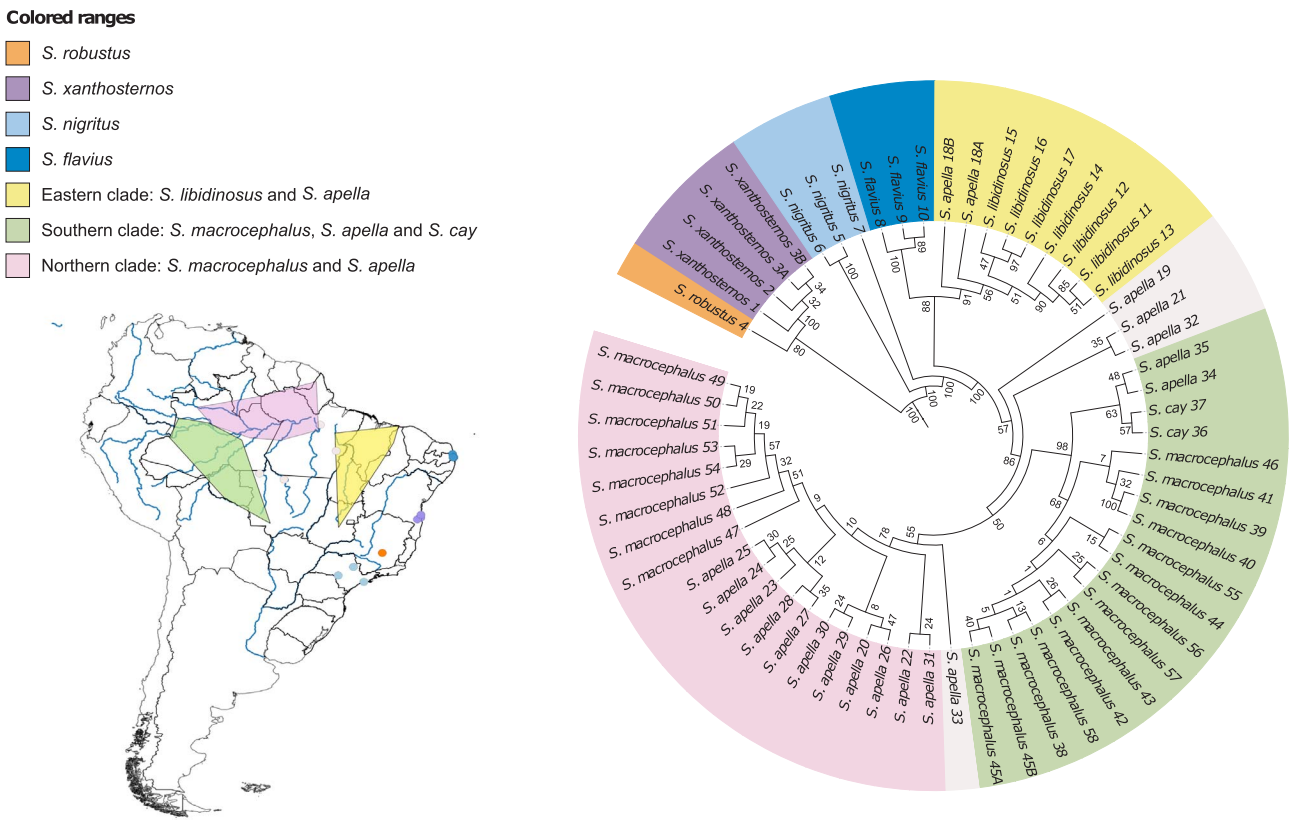

Fig. 3. Maximum likelihood for robust capuchin phylogeny based on SNPs data. Numbers next to nodes refer respectively to bootstrap values (based on 1000 replicates). Sample numbers correspond to those in Table 2 and Fig. 1. Inset map of South America displays minimum convex polygons to show geographic distribution of major subclades within the widespread *Sapajus* clade. *S. apella* samples 19, 21, 32, and 33 (light pink in the phylogeny and on the map) did not form part of any of the major subclades, probably due to extensive admixture in these samples (see Population genetic structure analyses below). (For interpretation of the references to color in this figure legend, the reader is referred to the web version of this article.)

(Fig. 3).

In the species tree recovered from SVDquartets (Fig. 4), the internal topology for *Sapajus* was congruent with our ML tree recovered using SNPs. As in other analyses, *Sapajus xanthosternos* and *S. robustus* were strongly supported as sister taxa (99). *S. apella*, *S. macrocephalus*, *S. cay*, *S. flavius*, and *S. libidinosus* formed a subclade (100) nested within the Atlantic forest robust capuchin clade and sister to *S. nigritus* (100). *S. flavius* was poorly supported (77) as sister to *S. libidinosus*, and Amazonian robust capuchins *S. apella, S. cay* and *S. macrocephalus* formed a clade together (98), with some support for *S. cay* as sister to *S. macrocephalus* (89).

3.4. Population genetic structure analyses

In the No Admixture analysis (K = 1–9) using STRUCTURE, we identified two major genetic clusters within *Sapajus*, as indicated by the highest value of delta K. These two clusters include (1) Atlantic Forest robust capuchins (*S. xanthosternos*, *S. robustus,* and *S. nigritus* 5 and 6); and (2) Cosmopolitan robust capuchins, from Amazonia, Pantanal, Cerrado, Caatinga and Atlantic Forest (*S. apella, S. macrocephalus, S. cay, S. libidinosus, S. flavius,* and *S. nigritus* sample 7). We further examined each of these two recovered clusters for substructure. For Atlantic Forest capuchins (*Sapajus xanthosternos*, *S. robustus*, *S. nigritus*), cluster analysis (K = 1–4) revealed most support for two clusters: (1) *S. xanthosternos* + *S. robustus*, and (2) *S. nigritus*. At K = 3, samples were clustered by species (*S. xanthosternos*; *S. robustus;* and *S. nigritus*). For the cosmopolitan capuchins, cluster analysis (K = 1–6) recovered two population clusters including: (1) a North Atlantic-Caatinga-Cerrado-East Amazon cluster (*S. flavius* + *S. libidinosus* + eastern *S. apella* from Tucuruí), and (2) a pan-Amazonia + Pantanal cluster (*S. apella, S. cay, S. macrocephalus*: Fig. 5).

In the Admixture run of STRUCTURE, we identified four genetic clusters within *Sapajus* (Fig. 6), as indicated by the highest value of delta K. Among these four clusters, there was evidence for three geographic regions with distinct 'pure' populations: *S. macrocephalus* (including *S. cay*) from south-central Amazonia, *S. libidinosus* from the northern Caatinga, and *S. xanthosternos* + *S. robustus* from the Atlantic Forest. All other geographic regions contained only admixed individuals. North of the Amazon River, all individuals were admixed from two populations ('*S. apella*' and '*S. macrocephalus*'), mostly with a higher proportion of *S. apella* ancestry. South of the Amazon River, following it west, *S. macrocephalus* ancestry increased to over 50% at around the Solimões River. *S. flavius*, *S. libidinosus* from the southern Cerrado, and *S. libidinosus* from the border of the Cerrado with Amazonia were all predominantly of '*libidinosus*' ancestry, but they are also all admixed, with some ancestry from *S. macrocephalus*. *S. nigritus* individuals are all admixed, each with different proportions of ancestry from *S. xanthosternos* + *robustus*; *S. libidinosus*; and *S. macrocephalus*. In general, the STRUCTURE analysis suggests high degrees of admixture across almost all 'species', with *S. macrocephalus* ancestry being the most widespread—throughout the Amazon, both north and south of the Amazon River, and as far as Northeast Brazil, the Cerrado, and the Southern Atlantic Forest.

In general, the Admixture analysis for population structuring pointed to a high index of gene flow both within and across ecosystems, and suggested that there are few regions in South America (or at least within Brazil, where the *Sapajus* samples originate for this study) with truly isolated populations of robust capuchin monkeys. The analysis suggests that interbreeding can occur across all morphotypes that come into contact. It also provides a novel explanation for why there is extremely high phenotypic diversity within populations, and why it has been difficult for morphologists to agree with confidence on

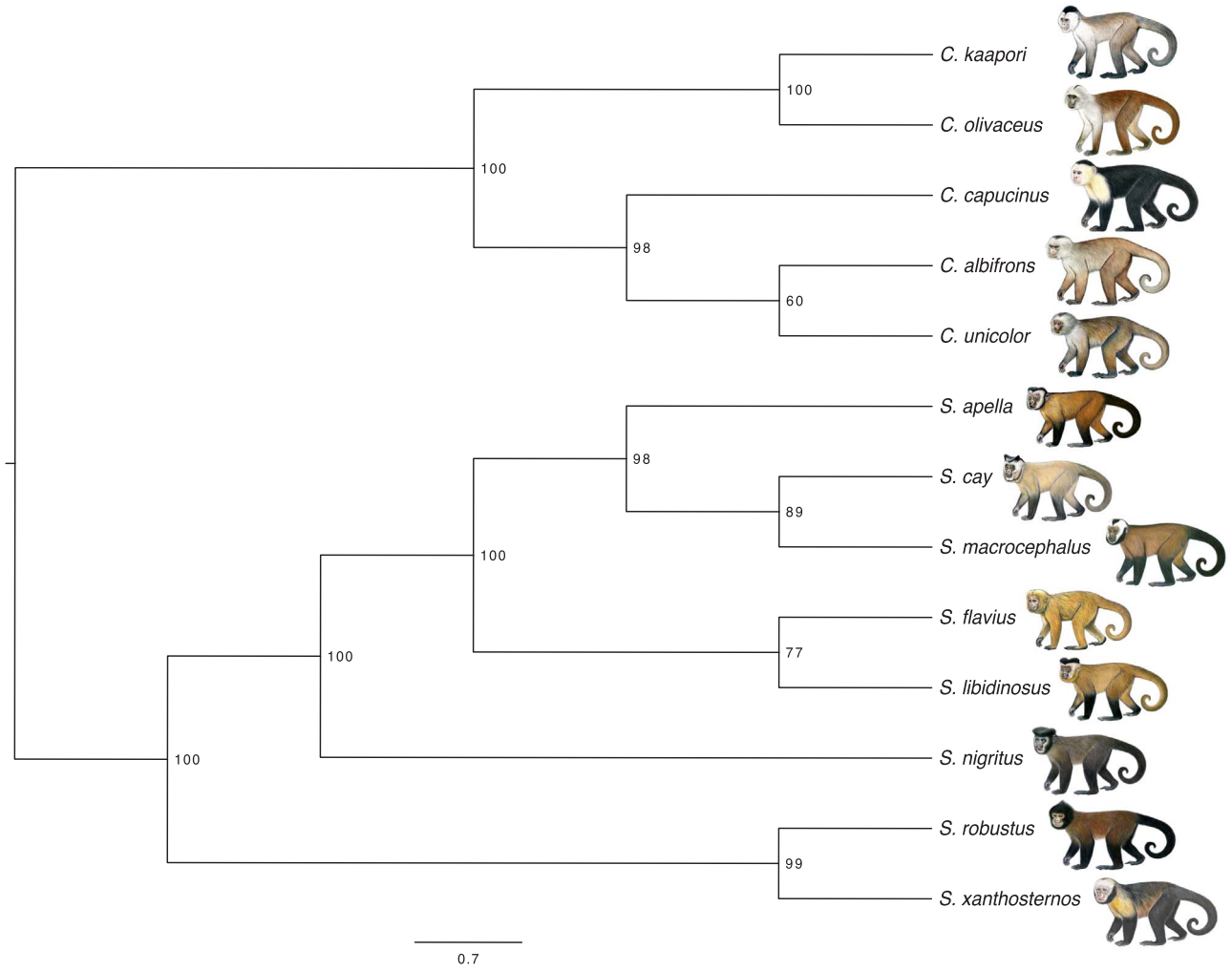

Fig. 4. Species tree for capuchin monkeys using SVDquartets. Numbers at each node represent the bootstrap support values. Illustrations by Stephen D. Nash/IUCN SSC Primate Specialist Group.

geographical dividing lines between different species.

3.5. Divergence time analyses

We found that the node age estimates generated by MCMCTree closely matched those inferred using BEAST, with the 95% highest posterior density (HPD) intervals largely overlapping for most nodes (Table 4). Both analyses placed the divergence between the two capuchin genera (node 17) in the Messinian stage of the late Miocene (MCMCTree: 7.0 Ma, BEAST: 6.5 Ma). The only discrepancy between the two methods concerned the age of the root, where MCMCTree yielded a posterior mean more than 50% older than the BEAST estimate (Table 4: node 20). This difference is likely to be explained by the different calibration densities assigned to the root. While the exponential density in BEAST concentrated most probability mass close to the minimum, the uniform density that had to be used for the MCMCTree analysis placed comparatively higher prior probability on older ages.

4. Discussion

Our SNP analyses provide genetic support for up to six distinct species within *Sapajus*: five species that are currently also recognized on the basis of morphological characteristics, plus one morphologically diverse and widespread lineage that occupies the Amazon and Pantanal regions of South America. Recent mitochondrial studies provided support for the species status of *S. robustus*, *S. xanthosternos*, and *S. nigritus*, although the exact relationships among these species were unresolved (Lima et al., 2017; Ruiz-Garcia et al., 2012). Our STRUCTURE analysis with no admixture matched well with Groves' (2001) taxonomy based on morphology, as both separated robust capuchins into a pan-Amazonian cluster (*S. apella*), a Caatinga/Cerrado cluster (*S. libidinosus*–samples from *S. flavius* were not included in Groves' study, but clustered with *S. libidinosus* in ours), and two Atlantic Forest clusters (*S. xanthosternos* and *S. nigritus*). However, our analysis placed *S. robustus* and *S. xanthosternos* in the same population cluster, with *S. nigritus* as a separate population cluster. In this aspect, both the mtDNA (Lima et al., 2017) and the nuclear DNA (this study) topologies are discordant with Groves' (2001) taxonomic hypothesis that considered *S. robustus* as a subspecies of *S. nigritus*, because *S. nigritus* and *S. robustus* do not group together as sister taxa within *Sapajus* in the molecular studies.

All *Sapajus libidinosus* samples with a light yellow pelage phenotype found across the relatively dry biomes of Caatinga and Cerrado cluster together in one clade. However, this clade also includes samples that represent standard *S. apella* pelage at the border of the two species distributions, near Tucuruí, Pará. Similarly, when using mitochondrial markers individuals with *S. apella* morphotypes from Tucuruí clustered genetically with all sampled individuals with *S. libidinosus* pelage from within *S. libidinosus*' distribution (Lima et al., 2017). Tucuruí capuchins have darker pelage and live in tropical forest habitat, while nearby *S. libidinosus* are adapted to open Cerrado and Caatinga habitats and have

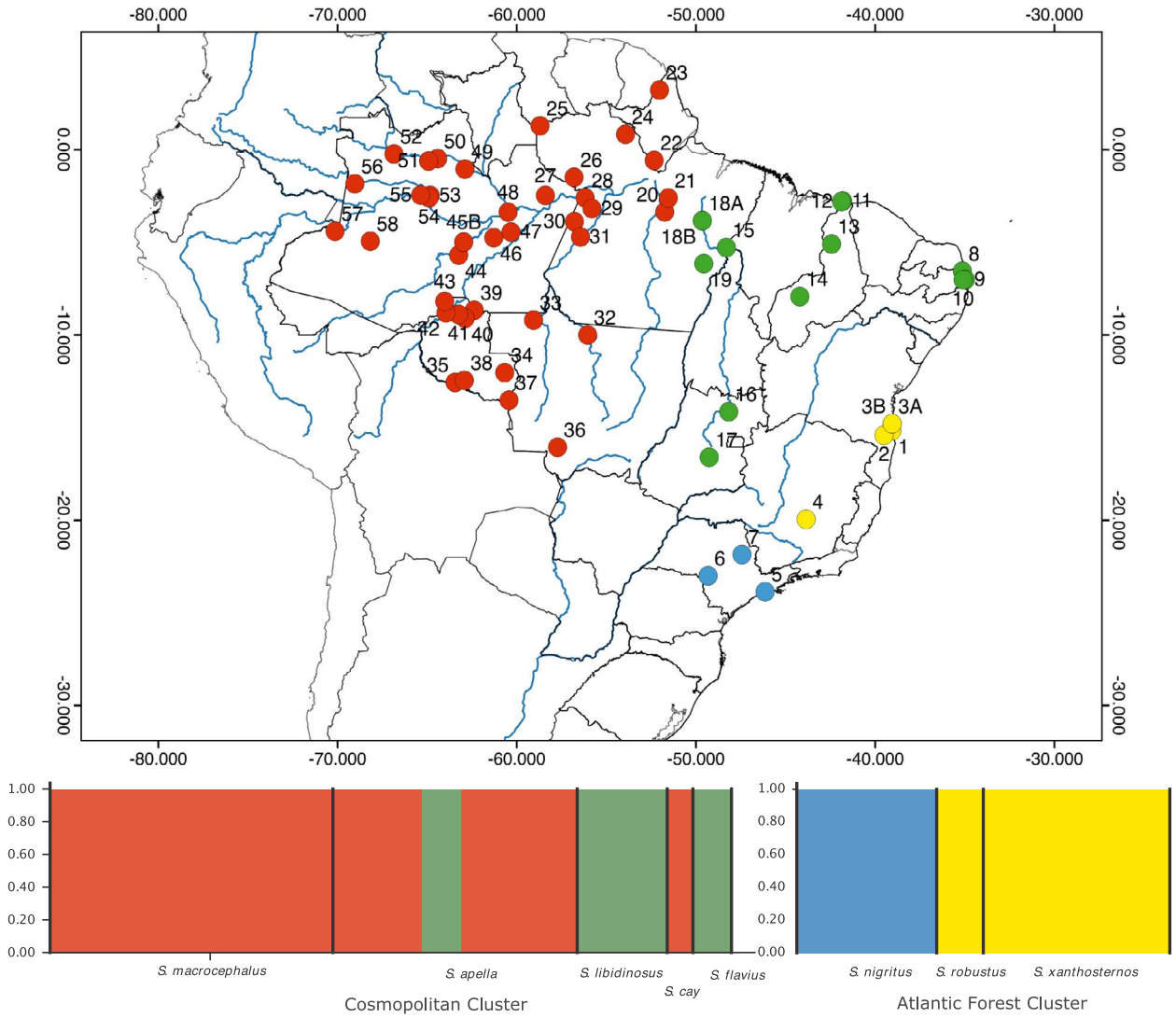

Fig. 5. Map showing geographic distribution for subclusters for the cosmopolitan robust capuchin cluster (red and green), and for the Atlantic Forest robust capuchin cluster (blue and yellow), each based on STRUCTURE plots for unlinked SNPs K = 2 using correlated frequency and No Admixture. Map sample numbers follow map localities from Fig. 1 and Table 2. (For interpretation of the references to color in this figure legend, the reader is referred to the web version of this article.)

lighter pelage. In our admixture analysis, the *S. libidinosus* individuals from the edge of the Cerrado have admixture with *S. apella,* and the *S. apella* individuals nearby have admixture with *S. libidinosus*. This suggests bidirectional gene flow, with natural selection maintaining the different phenotypes in the adjacent habitats.

Mitochondrial studies have recovered *S. flavius* as a monophyletic group, either embedded within the widespread Amazonian clade, or positioned as sister to that widespread clade (Lima et al., 2017), whereas results presented here using nuclear loci place *S. flavius* and *S. libidinosus* as sister taxa or as belonging to the same population cluster. In our SNPs tree, *Sapajus libidinosus* + Tucuruí samples formed a clade with *S. flavius*. *S. libidnosus* and *S. flavius* were indistinguishable from one another in the STRUCTURE analyses, both using Admixture (Fig. 6) or No Admixture (Fig. 5) models. More data from the Cerrado-Amazon transition zone and the Caatinga-Atlantic Forest transition zone could help resolve whether *S. flavius* and *S. libidinosus* are geographical variants of the same species, are two distinct species, or are best lumped within a widespread *Sapajus* species. Our admixture analysis reconstructs *S. flavius* as an admixed population, with about 80–90% ancestry from *S. libidinosus*, and 10–20% ancestry from *S. macrocephalus.*

The molecular distinctiveness of the other morphological species currently assigned to *Sapajus* is not supported. Within the widespread *Sapajus* clade recovered in the SNPs tree, there were strong indications for shared evolutionary history among the morphotypes *S. cay*, *S. apella*, and *S. macrocephalus*. We found no reciprocal monophyly between any of these morphologically defined taxa, and, instead, we observed geographic coherence for recovered lineages that did not correspond to current species hypotheses for Amazonian and Pantanal *Sapajus*. The pattern we see is in our STRUCTURE analyses is more concordant with multiple expansions across the Amazon and significant admixture across most Amazonian populations. Samples identified as *S. cay* formed a clade with geographically proximate *S. macrocephalus* samples, were identified as admixed, and were indistinguishable in their proportion of admixture from those for nearby *S. macrocephalus* samples. However, some studies have already indicated that *S. cay* from the Brazilian Pantanal and from Paraguay may not form a monophyletic group (Casado et al., 2010; Lima et al., 2017); we did not have Paraguayan samples in this study, so more work is needed on the full geographic range of *S. cay*.

Sapajus macrocephalus as defined by Rylands et al. (2013) is paraphyletic in our study. Samples collected north of the Solimões and

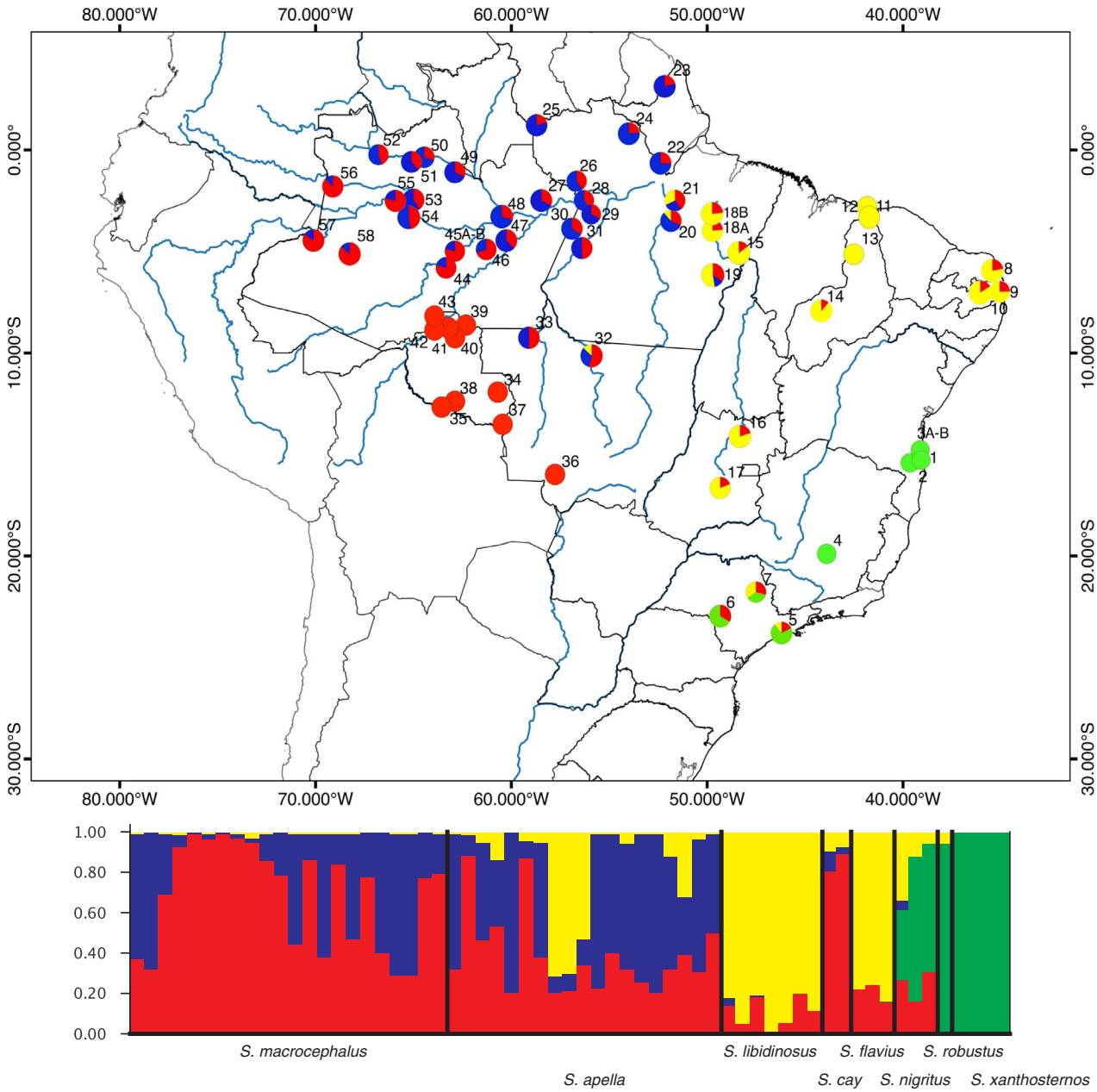

Fig. 6. STRUCTURE plot and map for all *Sapajus* SNPs K = 4 using correlated frequency and admixture. Filled circles on map represent individual ancestry based on cluster assignment, and when an individual is admixed from multiple clusters, the pie pieces represent the percentage ancestry from each cluster. Individuals are considered admixed only when at least 10% of their ancestry is attributed to a second (or third) cluster. Map sample numbers correspond to those in Table 2 and Fig. 1.

Japurá rivers and south of the Rio Negro group in the phylogeny with *S. apella* north of the Amazon (see Northern Clade in Fig. 3). In contrast, *S. macrocephalus* from south-central Amazonia south of the Solimões River is recovered in a clade with southern Amazonian *S. apella* and *S. cay* (Southern Clade, Fig. 3). In the admixture analysis, this discrepancy with morphology can be explained by high indices of admixture between source populations of *S. apella* and *S. macrocephalus*. All sampled *Sapajus* north of the Amazon River show significant admixture, and many individuals south of the Amazon River are also admixed between *S. apella* and *S. macrocephalus*. The proportion of *S. macrocephalus* ancestry increases on both sides of the Amazon River as one moves west across the continent, and the south-central Amazon basin includes 'pure' *S. macrocephalus* individuals. We recovered no 'pure' *S. apella* individuals from any localities in our study, but percentage of *S. apella* ancestry is highest in the north-east Amazon, closest to the type locality for *S. apella apella*, which is in the Guianas (Rylands et al., 2005).

Geographic boundaries and taxonomic affinities for *S. apella, S. cay*, *S. libidinosus*, and *S. macrocephalus* are disputed by the two predominant morphological authorities (Groves 2001, 2005; Silva-Júnior, 2001, 2002). For example, Groves (2001) considers *S. cay* as two distinct subspecies of *S. libidinosus* (called *Cebus libidinosus paraguayanus* and *Cebus libidinosus pallidus*), and treats *S. macrocephalus* as a subspecies of *S. apella* (*Cebus apella macrocephalus*). Neither mitochondrial (Lynch Alfaro et al., 2012a; Lima et al., 2017) nor nuclear data from the present study recovered reciprocal monophyly for *S. cay*, *S. apella*, or *S. macrocephalus*. We suggest that there are multiple 'source' populations of robust capuchin monkeys in the Amazon, but that rampant admixture makes it difficult to assign meaningful species boundaries here.

The time tree generated from our BEAST analysis (Table 4) placed the mean estimated divergence time for gracile and robust capuchins at 6.6 Ma. This is comparable to previous mean estimates for divergence between *Cebus* and *Sapajus* at 5.8 Ma, using mitochondrial data (Lima

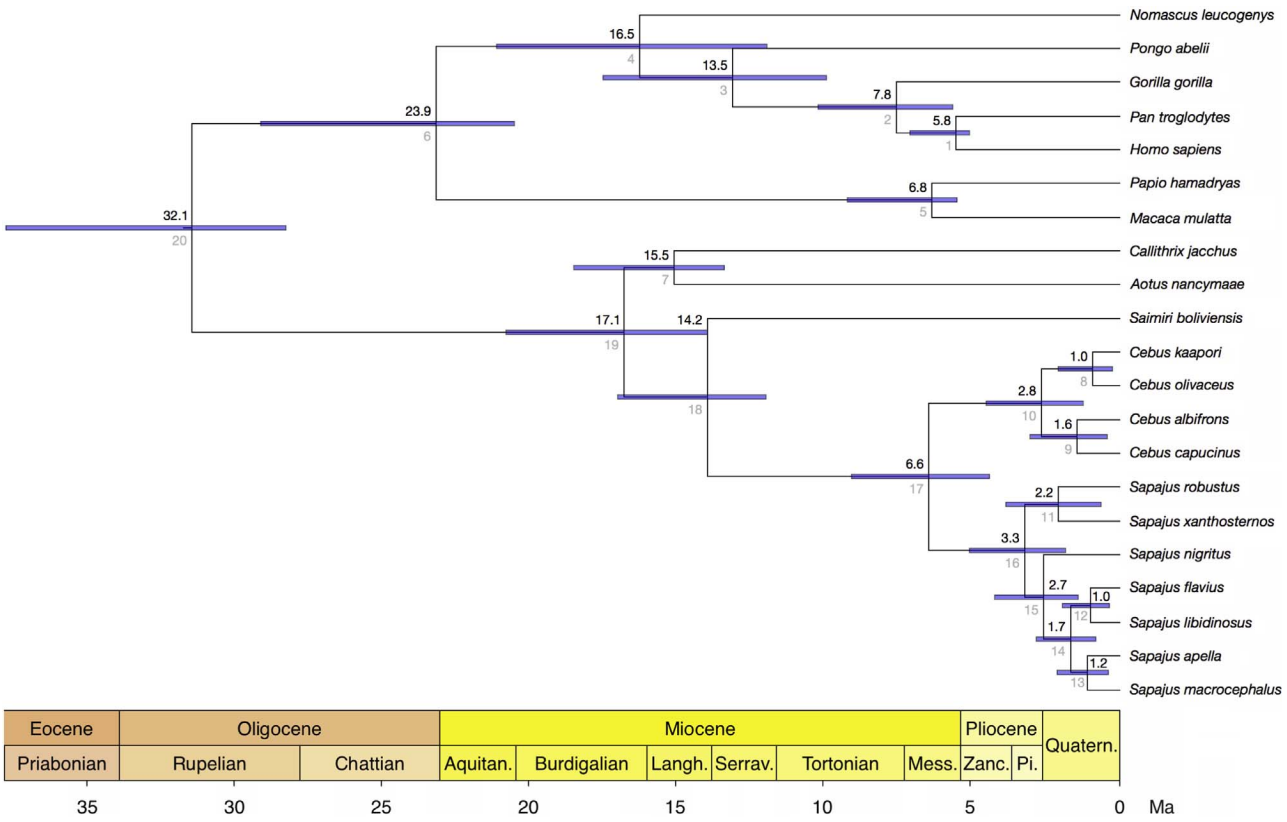

Fig. 7. BEAST time tree with node heights scaled to median divergence time estimates. Numbers in gray correspond to the node labels in Tables 3 and 4; numbers in black indicate the posterior means of the ages for each node. Blue bars represent 95% highest posterior density (HPD) intervals. (For interpretation of the references to color in this figure legend, the reader is referred to the web version of this article.)

Table 4
Summary of the posterior distribution of divergence times (in Ma) estimated using BEAST and MCMCTree (see Fig. 7 for node labels).

Node	BEAST		MCMCTree	
	Median	95% HPD	Mean	95% HPD
1	5.6	5.1–7.1	5.4	5.1–6.4
2	7.6	5.7–10.2	7.5	5.9–10.2
3	13.1	9.9–17.5	12.9	9.5–17.1
4	16.3	12.0–21.1	15.6	11.9–20.8
5	6.4	5.5–9.2	6.4	5.5–8.4
6	23.2	20.6–29.2	23.6	20.6–33.8
7	15.1	13.4–18.5	14.0	13.4–16.0
8	0.9	0.2–2.1	1.0	0.4–2.2
9	1.5	0.4–3.0	1.7	0.7–3.4
10	2.7	1.2–4.5	2.9	1.5–5.0
11	2.1	0.6–3.9	2.5	1.1–4.3
12	1.0	0.3–1.9	1.1	0.5–2.1
13	1.1	0.4–2.1	1.3	0.6–2.3
14	1.6	0.8–2.8	1.8	1.0–3.0
15	2.6	1.4–4.2	2.8	1.7–4.5
16	3.2	1.8–5.1	3.4	2.1–5.3
17	6.5	4.4–9.1	7.0	4.8–9.9
18	14.0	12.0–17.0	12.6	12.0–14.2
19	16.8	14.0–20.8	15.1	13.8–17.8
20	31.5	28.3–37.8	47.8	34.7–55.7

et al., 2017), at 6 Ma using a BEAST analysis for 54 nuclear genes (Perelman et al., 2011), and at 6.6 Ma for the MCMC tree in PAML utilizing autocorrelated rates and soft-bounded constraints for a supermatrix of both nuclear and mitochondrial genes (Springer et al., 2012). In other words, all analyses converge on a late Miocene divergence time for robust and gracile capuchin monkeys. This timing is consistent with the hypothesis that the formation of the savanna-like Cerrado led to vicariance of a widespread capuchin ancestor previously spanning the Amazon to the Atlantic Forest (Lynch Alfaro et al., 2015; Lima et al., 2017). The Amazon-Atlantic Forest splits for several other Neotropical primates were happening at about the same time period, suggesting vicariance through similar mechanisms for all of these arboreal primates (Amazonian *Lagothrix* versus Atlantic Forest *Brachyteles,* mean divergence time estimate from 8.6 to 11.3 Ma; Amazonian titi monkeys *Plecturocebus* versus Atlantic Forest titi monkeys *Callicebus*, mean divergence time estimate from 6.7 to 9.9 Ma; Amazonian marmosets *Mico* versus Atlantic Forest marmosets *Callithrix,* mean divergence time estimate 4.6–6.0 Ma, reviewed in Lynch Alfaro et al., 2015). While the drier climate and less hospitable ecosystem were likely the driving forces behind isolation of all of these monkeys in the Atlantic Forest versus the Amazon, in the last 1–2 Ma robust capuchins from the Atlantic Forest have colonized the Amazon, Cerrado, Caatinga, and Pantanal habitats, and we provide evidence for population admixture across the full range of these Neotropical habitats for this now cosmopolitan group.

5. Conclusions

Our phylogenomic data provides strong support for *Cebus* and *Sapajus* as two clades with a deep divergence date in the late Miocene. This is concordant with morphological evaluations of distinctiveness between robust and gracile capuchins (Elliot, 1913; Hershkovitz, 1949; Groves, 2001, 2005; Silva-Júnior, 2001, 2002; Lynch Alfaro et al., 2012b), and with mitochondrial and *Alu* element data that also point to this split (Lynch Alfaro et al., 2012a; Lima et al., 2017; Martins Jr. et al., 2015; Viana et al., 2015). In our BEAST analysis, the median estimate for the initial diversification of robust capuchins was at 3.3 Ma; this late Pliocene diversification is somewhat earlier than previous studies using mitochondrial data (Lynch Alfaro et al. 2012a; Lima et al., 2017).

In general, our phylogenies based on ultraconserved elements were congruent with mitochondrial phylogenies for robust capuchins (Lynch Alfaro et al., 2012a, 2012b; Lima et al., 2017), although the placement of *S. robustus* as sister to *S. xanthosternos* was unique to the nuclear phylogenomic data, as was the recovery of a sister relationship between *S. flavius* and *S. libidinosus*. Our UCE tree distinguished only four *Sapajus* species, but the ML SNPs tree provided more support for six robust capuchin species, *S. xanthosternos*, *S. robustus*, *S. nigritus*, *S. flavius*, *S. libidinosus*, and a widespread Amazonian and Pantanal species. The major division within the Amazonian robust capuchins, according to molecular phylogenomics, is a Northeast-Southwest division (both in the present work and from mitochondrial data in Lima et al., 2017), whereas the morphological division of *S. macrocephalus* and *S. apella* has been described as more of an East-West division, with the Madeira and Negro rivers as the suggested dividing line (Groves, 2001, 2005; Silva-Júnior, 2001, 2002). Difficulty in assigning species by morphology or phylogeny may be a result of widespread population admixture facilitated through frequent movement across major rivers and even ecosystems by robust capuchin monkeys. Morphological and phylogenetic subdivisions of the Amazonian group are discordant, which in large part can be explained by the high indices of admixture across populations. However, this does not discount the importance of population differences in behavior, morphology and ecology in capuchins across the Amazon, southern Cerrado and Pantanal; these differences may serve as a model for understanding the rapid evolution of divergent phenotypes across diverse habitats in other highly polymorphic taxa, such as humans.

Acknowledgments

Special thanks to Stephen D. Nash/IUCN SSC Primate Specialist Group for illustrations, copyright 2013, and to Brant Faircloth for generous and helpful advice on all things related to UCEs. Thanks to Amanda Melin, Katharine Jack, and Gustavo Gutiérrez-Espeleta for providing gracile capuchin samples. Support to M.G.M.L.'s PhD research was provided by a CNPq PhD fellowship (142141/2012-7) and CNPq SWE fellowship (201172/2014-3). Some of the field expeditions were funded by CNPq/FAPEAM SISBIOTA Program (563348/2010-0) to J.P.B. UCE data was generated with support from NSF-FAPESP (grant 1241066 – Dimensions US-BIOTA-São Paulo: Assembly and evolution of the Amazonian biota and its environment: an integrated approach) to A.A. Divergence time analyses were performed with support from the Whitcome Research Fellowship to D.Č. Thanks to two anonymous reviewers whose comments greatly improved our work.

Appendix A. Supplementary material

Supplementary data associated with this article can be found, in the online version, at https://doi.org/10.1016/j.ympev.2018.02.023.

References

Barba-Montoya, J., dos Reis, M., Yang, Z., 2017. Comparison of different strategies for using fossil calibrations to generate the time prior in Bayesian molecular clock dating. Mol. Phylogenet. Evol. 114, 386–400.

Benton, M.J., Donoghue, P.C.J., 2007. Paleontological evidence to date the tree of life. Mol. Biol. Evol. 24, 26–53.

Bloch, J.I., Woodruff, E.D., Wood, A.R., Rincon, A.F., Harrington, A.R., Morgan, G.S., Foster, D.A., Montes, C., Jaramillo, C.A., Jud, N.A., Jones, D.S., MacFadden, B.J., 2016. First North American fossil monkey and early Miocene tropical biotic interchange. Nature 533, 243–246.

Bolger, A.M., Lohse, M., Usadel, B., 2014. Trimmomatic: a flexible trimmer for illumina sequence data. Bioinformatics 30, 2114–2120.

Cabrera, A., 1957. Catálogo de los mamíferos de América del Sur. I (Metatheria, Unguiculata, Carnívora). Rev. Mus. Argentino Cien. Nat Cien. Zool. 4, 1–307.

Casado, F., Bonvicino, C.R., Nagle, C., Comas, B., Manzur, T.D., Lahoz, M.M., Seuánez, H.N., 2010. Mitochondrial divergence between 2 populations of the hooded capuchin, *Cebus* (*Sapajus*) *cay* (Platyrrhini, Primates). J. Hered. 101, 261–269. http://dx.doi.org/10.1093/jhered/esp119.

Chifman, J., Kubatko, L., 2014. Quartet inference from SNP data under the coalescent model. Bioinformatics 30, 3317–3324. http://dx.doi.org/10.1093/bioinformatics/btu530.

Cole, T.M., 1992. Postnatal heterochrony of the masticatory apparatus in *Cebus apella* and *Cebus albifrons*. J. Hum. Evol. 23 (3), 253–282.

Crawford, N.G., Faircloth, B.C., McCormack, J.E., Brumfield, R.T., Winker, K., Glenn, T.C., 2012. More than 1000 ultraconserved elements provide evidence that turtles are the sister group of archosaurs. Biol. Lett. 8, 783–786. http://dx.doi.org/10.1098/rsbl.2012.0331.

Daegling, D.J., 1992. Mandibular morphology and diet in the genus *Cebus*. Int. J. Primatol. 13, 545–570. http://dx.doi.org/10.1007/BF02547832.

Danecek, P., Auton, A., Abecasis, G., Albers, C.A., Banks, E., DePristo, M.A., Handsaker, R.E., Lunter, G., Marth, G.T., Sherry, S.T., McVean, G., Durbin, R., 2011. The variant call format and VCF tools. Bioinformatics 27, 2156–2158. http://dx.doi.org/10.1093/bioinformatics/btr330.

Drummond, A.J., Suchard, M.A., Xie, D., Rambaut, A., 2012. Bayesian phylogenetics with BEAUTi and the BEAST 1.7. Mol. Biol. Evol. 29, 1969–1973. http://dx.doi.org/10.1093/molbev/mss075.

Earl, D.A., vonHoldt, B.M., 2012. STRUCTURE HARVESTER: a website and program for visualizing STRUCTURE output and implementing the Evanno method. Conserv. Genet. Resour. 4 (2), 359–361.

Elliot, D.G., 1913. A Review of Primates. Monograph Series. American Museum of Natural History, New York.

Evanno, G., Regnaut, S., Goudet, J., 2005. Detecting the number of clusters of individuals using the software STRUCTURE: a simulation study. Mol. Ecol. 14, 2611–2620.

Faircloth, B.C., McCormack, J.E., Crawford, N.G., Harvey, M.G., Brumfield, R.T., Glenn, T.C., 2012. Ultraconserved elements anchor thousands of genetic markers spanning multiple evolutionary timescales. Syst. Biol. 61, 717–726. http://dx.doi.org/10.1093/sysbio/sys004.

Faircloth, B.C., 2013. Illumiprocessor: a trimmomatic wrapper for parallel adapter and quality trimming. http://dx.doi.org/10.6079/J9ILL.

Faircloth, B.C., 2016. PHYLUCE is a software package for the analysis of conserved genomic loci. Bioinformatics 32, 786–788. http://dx.doi.org/10.6084/m9.figshare.1284521.Contact.

Faircloth, B.C., Sorenson, L., Santini, F., Alfaro, M.E., 2013. A phylogenomic perspective on the radiation of ray-finned fishes based upon targeted sequencing of ultraconserved elements (UCEs). PLoS One 8, e65923. http://dx.doi.org/10.1371/journal.pone.0065923.

Ford, S.M., Hobbs, D.G., 1996. Species Definition and Differentiation as Seen in the Postcranial Skeleton of *Cebus*. In: Norconk, M.A., Rosenberger, A.L., Garber, P.A. (Eds.), Adaptive Radiations of Neotropical Primates. Plenum Press, New York, pp. 229–249.

Fragaszy, D., Visalberghi, E., Fedigan, L., 2004. The Complete Capuchin. Cambridge University Press, Cambridge, pp. 339.

Frandsen, P.B., Calcott, B., Mayer, C., Lanfear, R., 2015. Automatic selection of partitioning schemes for phylogenetic analyses using iterative *k*-means clustering of site rates. BMC Evol. Biol. 15, 13. http://dx.doi.org/10.1186/s12862-015-0283-7.

Gernhard, T., 2008. The conditioned reconstructed process. J. Theor. Biol. 253, 769–778. http://dx.doi.org/10.1016/j.jtbi.2008.04.005.

Giarla, T.C., Esselstyn, J.A., 2015. The challenges of resolving a rapid, recent radiation: empirical and simulated phylogenomics of Philippine Shrews. Syst. Biol. 64, 727–740.

Groves, C.P., 2001. Primate Taxonomy. Smithsonian Institution Press, Washington, DC.

Groves, C.P., 2005. Order Primates. In: Wilson, D.E., Reeder, D.M. (Eds.), Mammal Species of the World: A Taxonomic and Geographic Reference, third ed., vol. 1. Johns Hopkins University Press, Baltimore, MD, pp. 111–184.

Haile-Selassie, Y., 2001. Late Miocene hominids from the middle Awash, Ethiopia. Nature 412, 178–181.

Harris, R.S., 2007. Improved Pairwise Alignment of Genomic DNA. The Pennsylvania State University Ph.D. Thesis.

Hershkovitz, P., 1949. Mammals of northern Colombia. Preliminary report N. 4: monkeys (Primates), with taxonomic revisions of some forms. Proc. United States Natl. Museum. 98, 323–427.

Hill, W.C.O., 1960. Primates: Comparative Anatomy and Taxonomy. IV. Cebidae, Part A. Interscience, New York.

IUCN, 2017. The IUCN Red List of Threatened Species. Version 2017-1. < http://www.iucnredlist.org > (Downloaded on 19 June 2017).

Kappelman, J., Kelley, J., Pilbeam, D., Sheikh, K.A., Ward, S., Anwar, M., Barry, J.C., Brown, B., Hake, P., Johnson, N.M., Raza, S.M., Ibrahim Shah, S.M., 1991. The earliest occurrence of *Sivapithecus* from the middle Miocene Chinji formation of Pakistan. J. Human Evol. 21, 61–73.

Katoh, K., Standley, D.M., 2013. MAFFT multiple sequence alignment software version 7: improvements in performance and usability. Mol. Biol. Evol. 30, 772–780. http://dx.doi.org/10.1093/molbev/mst010.

Kay, R.F., 2015. Biogeography in deep time – what do phylogenetics, geology, and paleoclimate tell us about early platyrrhine evolution? Mol. Phylogenet. Evol. 82, 358–374. http://dx.doi.org/10.1016/j.ympev.2013.12.002.

Köhler, M., Moyà-Solà, S., Alba, D.M., 2000. *Macaca* (Primates, Cercopithecidae) from the Late Miocene of Spain. J. Human Evol. 38, 447–452.

Lanfear, R., Calcott, B., Ho, S.Y.W., Guindon, S., 2012. PartitionFinder: combined selection of partitioning schemes and substitution models for phylogenetic analyses. Mol. Biol. Evol. 29, 1695–1701. http://dx.doi.org/10.1093/molbev/mss020.

Lanfear, R., Frandsen, P.B., Wright, A.M., Senfeld, T., Calcott, B., 2017. PartitionFinder 2: New methods for selecting partitioned models of evolution for molecular and morphological phylogenetic analyses. Mol. Biol. Evol. 34, 772–773. http://dx.doi.org/10.1093/molbev/msw260.

Lanfear, R., Calcott, B., Kainer, D., Mayer, C., Stamatakis, A., 2014. Selecting optimal

partitioning schemes for phylogenomic datasets. BMC Evol. Biol. 14, 82. http://dx.doi.org/10.1186/1471-2148-14-82.
Li, H., Durbin, R., 2009. Fast and accurate short read alignment with Burrows-Wheeler transform. Bioinformatics 25, 1754–1760. http://dx.doi.org/10.1093/bioinformatics/btp324.
Lima, M.G.M., Buckner, J.C., Silva-Júnior, J.de S.e., Aleixo, A., Martins, A.B., Boubli, J.P., Link, A., Farias, I.P., da Silva, M.N., Röhe, F., Queiroz, H., Chiou, K.L., Di Fiore, A., Alfaro, M.E., Lynch Alfaro, J.W., 2017. Capuchin monkey biogeography: understanding *Sapajus* Pleistocene range expansion and the current sympatry between *Cebus* and *Sapajus*. J. Biogeogr. 1–11. http://dx.doi.org/10.1111/jbi.12945.
Lynch Alfaro, J.W., Boubli, J.P., Olson, L.E., Di Fiore, A., Wilson, B., Gutiérrez-Espeleta, G.A., Chiou, K.L., Schulte, M., Neitzel, S., Ross, V., Schwochow, D., Nguyen, M.T.T., Farias, I., Janson, C.H., Alfaro, M.E., 2012a. Explosive Pleistocene range expansion leads to widespread Amazonian sympatry between robust and gracile capuchin monkeys. J. Biogeogr. 39, 272–288.
Lynch Alfaro, J.W., Silva-Junior, J.S., Rylands, A.B., 2012b. How different are robust and gracile capuchin monkeys? An argument for the use of *Sapajus* and *Cebus*. Am. J. Primatol. 74, 273–286.
Lynch Alfaro, J.W., Izar, P., Ferreira, R.G., 2014. Capuchin monkey research priorities and urgent issues. Am. J. Primatol. 76, 705–720. http://dx.doi.org/10.1002/ajp.22269.
Lynch Alfaro, J.W., Cortés-Ortiz, L., Di Fiore, A., Boubli, J.P., 2015. Special issue: comparative biogeography of Neotropical primates. Mol. Phylogenet. Evol. 82, 518–529. http://dx.doi.org/10.1016/j.ympev.2014.09.027.
Martins Jr., A.M.G., Amorim, N., Carneiro, J.C., de Mello Affonso, P.R.A., Sampaio, I., Schneider, H., 2015. Alu elements and the phylogeny of capuchin (*Cebus* and *Sapajus*) monkeys. Am. J. Primatol. 77, 368–375. http://dx.doi.org/10.1002/ajp.22352.
Masterson, T.J., 1997. Sexual dimorphism and interspecific cranial form in two capuchin species: *Cebus albifrons* and *C. apella*. Am. J. Phys. Anthropol. 104, 487–511. http://dx.doi.org/10.1002/(SICI)1096-8644(199712)104:4<487::AID-AJPA5>3.0.CO;2-P.
McCormack, J.E., Faircloth, B.C., Crawford, N.G., Gowaty, P.A., Brumfield, R.T., Glenn, T.C., 2012. Ultraconserved elements are novel phylogenomic markers that resolve placental mammal phylogeny when combined with species-tree analysis. Genome Res. 22, 746–754. http://dx.doi.org/10.1101/gr.125864.111.
McCormack, J., Tsai, W.L.E., Faircloth, B.C., 2015. Sequence capture of ultraconserved elements from bird museum specimens. Mol. Ecol. Resour. 1–15. http://dx.doi.org/10.1101/020271.
McKenna, A., Hanna, M., Banks, E., Sivachenko, A., Cibulskis, K., Kernytsky, A., Garimella, K., Altshuler, D., Gabriel, S., Daly, M., DePristo, M.A., 2010. The genome analysis toolkit: a MapReduce framework for analyzing next-generation DNA sequencing data. Genome Res. 20, 1297–1303. http://dx.doi.org/10.1101/gr.107524.110.
Perelman, P., Johnson, W.E., Roos, C., Seuánez, H.N., Horvath, J.E., Moreira, M.A.M., Kessing, B., Pontius, J., Roelke, M., Rumpler, Y., Schneider, M.P.C., Silva, A., O'Brien, S.J., Pecon-Slattery, J., 2011. A molecular phylogeny of living primates. PLoS Genet. 7, e1001342. http://dx.doi.org/10.1371/journal.pgen.1001342.
Perez, S.I., Rosenberger, A.L., 2014. The status of platyrrhine phylogeny: a meta-analysis and quantitative appraisal of topological hypotheses. J. Human Evol. 76, 177–187.
Pritchard, J.K., Stephens, M., Donnelly, P., 2000. Inference of population structure using multilocus genotype data. Genetics 155, 945–959.
Rambaut, A., Drummond, A.J., Suchard, M., 2013. Tracer v1.6. Available from < http://tree.bio.ed.ac.uk/software/tracer/ > .
Rambaut, A., Drummond, A.J., 2015. TreeAnnotator v1.8.4. Available from < http://beast.bio.ed.ac.uk/downloads/ >
Ruiz-García, M., Castillo, M.I., Lichilín-Ortiz, N., Pinedo-Castro, M., 2012. Molecular relationships and classification of several tufted capuchin lineages (*Cebus apella, Cebus xanthosternos* and *Cebus nigritus*, Cebidae), by means of mitochondrial cytochrome oxidase II gene sequence. Folia Primatol. 83, 100–125. http://dx.doi.org/10.1159/000342832.
Rylands, A.B., Mittermeier, R.A., 2009. The diversity of the New World primates (Platyrrhini): An annotated taxonomy. In: Garber, P.A., Estrada, A., Bicca-Marques, J.C., Heymann, E.W., Strier, K.B. (Eds.), South American Primates: Comparative Perspectives in the Study of Behavior, Ecology and Conservation. Springer Science +Business Media LLC, pp. 23–54.
Rylands, A.B., Mittermeier, R.A., 2014. Primate taxonomy: species and conservation. Evol. Anthropol. 23, 8–10.
Rylands, A., Kierulff, M., Mittermeier, R., 2005. Notes on the taxonomy and distributions of the tufted capuchin monkeys (*Cebus*, Cebidae) of South America. Lundiana 6, 97–110.
Rylands, A.B., Mittermeier, R.A., Silva-Júnior, J.S., 2012. Neotropical primates: taxonomy and recently described species and subspecies. Int. Zoo Yearb. 46, 11–24.
Rylands, A.B., Mittermeier, R.A., Bezerra, B.M., Paim, F.P., Queiroz, H.L., 2013. Species accounts of Cebidae. In: In: Mittermeier, R.A., Rylands, A.B., Wilson, D.E. (Eds.), Handbook of the Mammals of the World, vol. 3. Primates. Lynx Edicions, Barcelona, pp. 390–413.
Silva-Júnior, J.S., 2001. Especiação nos Macacos-prego e Caiararas, Gênero Cebus Erxleben, 1777 (Primates, Cebidae). Universidade Federal do Rio de Janeiro, Rio de Janeiro PhD Thesis.
Silva-Júnior, J.S., 2002. Taxonomy of capuchin monkeys, *Cebus* Erxleben, 1777. Neotrop. Primates 10, 29.
Silva-Júnior, J.S., 2005. Especiação nos Macacos-prego e Caiararas, gênero *Cebus* Erxleben, 1777 (Primates, Cebidae). Bol. Soc. Bras. Mastoz. 42, 11–12.
Springer, M.S., Meredith, R.W., Gatesy, J., Emerling, C.A., Park, J., Rabosky, D.L., Stadler, T., Steiner, C., Ryder, O.A., Janečka, J.E., Fisher, C.A., Murphy, W.J., 2012. Macroevolutionary dynamics and historical biogeography of primate diversification inferred from a species supermatrix. PLoS One 7, e49521. http://dx.doi.org/10.1371/journal.pone.0049521.
Stamatakis, A., 2014. RAxML version 8: a tool for phylogenetic analysis and post-analysis of large phylogenies. Bioinformatics 30, 1312–1313. http://dx.doi.org/10.1093/bioinformatics/btu033.
Swofford, D.L., 2002. PAUP*. Phylogenetic Analysis Using Parsimony (*and Other Methods). version 4. Sinauer Associates, Sunderland, Massachusetts.
Torres de Assumpção, C., 1983. An ecological study of the primates of southeastern Brazil, with a reappraisal of *Cebus apella* races (PhD Thesis). University of Edinburgh, Edinburgh.
Viana, M.C., Menezes, A.N., Moreira, M.A.M., Pissinatti, A., Seuánez, H.N., 2015. MECP2, a gene associated with Rett syndrome in humans, shows conserved coding regions, independent Alu insertions, and a novel transcript across primate evolution. BMC Genet. 16, 77. http://dx.doi.org/10.1186/s12863-015-0240-x.
Wright, B.W., 2005a. Craniodental biomechanics and dietary toughness in the genus *Cebus*. J. Hum. Evol. 48, 473–492. http://dx.doi.org/10.1016/j.jhevol.2005.01.006.
Wright, K.A., 2005b. Interspecific and ontogenetic variation in locomotor behavior, habitat use, and postcranial morphology in *Cebus apella* and *Cebus olivaceus*. Northwestern University, Evanston (IL), pp. 433 dissertation.
Wright, K.A., 2007. The relationship between locomotor behavior and limb morphology in brown (*Cebus apella*) and weeper (*Cebus olivaceus*) capuchins. Am. J. Primatol. 69, 736–756. http://dx.doi.org/10.1002/ajp.20391.
Yang, Z., 2007. PAML 4: phylogenetic analysis by maximum likelihood. Mol. Biol. Evol. 24, 1586–1591.
Yang, Z., 2017. User guide: PAML: phylogenetic analysis by maximum likelihood. Version 4.9d (February 2017). Available from < http://abacus.gene.ucl.ac.uk/software/pamlDOC.pdf > .
Young, N.M., MacLatchy, L., 2004. The phylogenetic position of *Morotopithecus*. J. Human Evol. 46, 163–184.